The Journal of Experimental Biology 200, 3109–3118 (1997)
Printed in Great Britain © The Company of Biologists Limited 1997
JEB0985



# ENDOCARDIAL ENDOTHELIUM IN THE AVASCULAR HEART OF THE FROG: MORPHOLOGY AND ROLE OF NITRIC OXIDE

STANISLAS U. SYS[1], DANIELA PELLEGRINO[2], ROSA MAZZA[2], ALFONSINA GATTUSO[2], LUC J. ANDRIES[1] AND BRUNO TOTA[2,3,*]

[1]*Laboratory of Human Physiology and Pathophysiology, University of Antwerp (RUCA), 2020 Antwerp, Belgium,* [2]*Dipartimento di Biologia Cellulare, Università della Calabria, 87030 Arcavacata di Rende (CS), Italy* and [3]*Stazione Zoologica 'A. Dohrn', Villa Comunale, I-80121 Napoli, Italy*

*Accepted 30 September 1997*

## Summary

**Endocardial endothelial morphology and the physiological modulatory role of nitric oxide (NO) were studied in an *in vitro* preparation of the working intact heart of the frog *Rana esculenta*, which lacks coronary vasculature and is thus devoid of a coronary vascular endothelium. *En face* confocal scanning laser microscopy of samples of perfused fixed hearts demonstrated the presence of NO synthase as a cytoplasmic constituent of the endocardial endothelial cells. Stroke volume (as a measure of performance in paced frog hearts) and stroke work (as an index of systolic function) increased by approximately 5 % after inhibition of the NO–cGMP pathway with $10^{-4}$ mol $l^{-1}$ $N^{G}$-nitro-L-arginine methyl ester and by approximately 8 % after inhibition with $10^{-6}$ mol $l^{-1}$ Methylene Blue. In contrast, stroke volume and stroke work decreased by approximately 22 % after activation of the NO–cGMP pathway with sodium nitroprusside ($10^{-4}$ mol $l^{-1}$), while 3-morpholinosydnonimine ($5\times10^{-8}$ to $10^{-5}$ mol $l^{-1}$) caused a decrease of between 15 and 30 % and 8-bromo-cGMP ($10^{-6}$ mol $l^{-1}$) a decrease of approximately 8 %. These responses were significantly attenuated after exposure of the ventricular luminal to Triton X-100 (0.05 %, 0.1 ml), which itself increased performance (by over 10 %) without detectable morphological changes. These results show that the endocardial endothelium of *Rana esculenta* produces amounts of NO sufficient to modulate ventricular performance.**

Key words: endocardial endothelium, nitric oxide, cyclic GMP, myocardial performance, frog, heart, *Rana esculenta*.

## Introduction

The endocardial endothelium (EE), strategically located between the superfusing luminal blood and the underlying cardiac musculature, plays an obligatory role in controlling myocardial performance in various mammalian species in a manner analogous to the autocrine–paracrine autoregulation of smooth muscle by vascular endothelium (Brutsaert and Andries, 1992; Brutsaert *et al.* 1988; Smith *et al.* 1991). The endothelium of the coronary (micro)vasculature has also been found to regulate myocardial performance (Brutsaert *et al.* 1996). The secretory function of the EE involves the synthesis and release of NO and of other autacoids including prostacyclin and endothelin.

Although both microvascular coronary and endocardial endothelial cells produce common autacoids and share similar roles in the signal transduction initiated by circulating hormones, neurotransmitters or mechanical stimuli, they clearly represent two cell populations with distinct embryological origin and morphological and functional characteristics. To what extent the interactions between myocardium, microvascular coronary endothelium and EE are integrated in cardiac homeostasis and the mechanisms involved are the subject of intensive investigation. In mammalian cardiac muscle preparations, evaluation of the specific role of the EE is hampered by the coexistence of the microvascular coronary endothelium. In contrast, amphibians such as the frog possess an avascular heart, i.e. the myocardium is totally trabeculated and is supplied by luminal blood solely through the intertrabecular spaces (i.e. lacunae) (Grant and Regnier, 1926; Staley and Benson, 1968). Given the fully trabeculated wall of the ventricle and the correspondingly very high ratio of cavity surface to ventricular volume, the EE in the frog has a relatively greater mass than the EE in the compact type of ventricular myoarchitecture in mammals. The frog heart can, therefore, be used to study direct interactions between the EE and myocardium in the whole working heart, without interference from a microvascular coronary endothelium.

The aim of this paper was to explore the potential of using an avascular heart to study the role of the EE. We investigated the morphological features of the EE in the heart of *Rana esculenta* with particular reference to the presence of the

*Author for correspondence at address 3 (e-mail: tota@pobox.unical.it).

constitutive form of NO synthase (cNOS). Because the EE of the intact working heart is continuously exposed to physical forces associated with blood flow, we used an *in vitro* isolated and perfused frog heart preparation working at physiological haemodynamic loads (Acierno *et al.* 1994) to analyse the functional role of the EE in relation to cNOS activity.

## Materials and methods

### *The isolated and perfused working heart preparation*

Frog hearts ($N$=104) were isolated from specimens of both sexes of *Rana esculenta* (weighing 20.8±0.7 g; mean value ± S.E.M.) and connected to a perfusion apparatus as previously described (Acierno *et al.* 1994). Experiments were carried out at room temperature (18–21 °C) from autumn to spring. In electrically paced heart preparations, a Grass S44 stimulator was used (single pulses of 20 V, 0.1 s) with a stimulation rate identical to the control (unpaced) rate. The saline composition was (in mmol $l^{-1}$): NaCl, 115; KCl, 2.5; $CaCl_2$, 1.0; $Na_2HPO_4$, 2.15; $NaH_2PO_4$, 0.85; anhydrous glucose, 5.6; pH was adjusted to 7.2 by adding $Na_2HPO_4$. The final molarity was 2.46 mmol $l^{-1}$ (Singh and Flitney, 1981). The saline was equilibrated with air. The mean input pressure (preload) was regulated by varying the height of the input reservoir in relation to the level of the atrium, and the minimal output pressure (afterload) was similarly controlled by adjusting the reservoir height with respect to the aortic trunk.

### *Measurements and calculations*

Pressure measurements were made through T-tubes placed immediately before the input cannula and after the output cannula, and connected to two MP-20D pressure transducers (Micron Instruments, Simi Valley, CA, USA) in conjunction with a Unirecord 7050 (Ugo Basile, Comerio, Italy). Pressure measurements were expressed in kPa and corrected for cannula resistance. Heart rate was calculated from pressure recording curves. Cardiac output was collected over 1 min and weighed; values were corrected for temperature and fluid density and expressed as volumes. Cardiac output ($\dot{Q}$) and stroke volume ($V_S$=$\dot{Q}$/heart rate) were normalized per kilogram of wet body mass. Stroke volume at constant pre- and afterload in paced hearts was used as a measure of ventricular performance; changes in stroke volume under these conditions were considered inotropic effects. Ventricular stroke work ($W_S$) was calculated in mJ $g^{-1}$ as (afterload − preload × stroke volume)/ventricle mass. The duration of the systolic phase (see Fig. 3A) was calculated from recording traces.

### *Experimental protocols*

#### *Establishing basal conditions and drug application*

In all experiments, hearts were initially allowed to maintain a spontaneous rhythm. The afterload pressure was set at 3.92 kPa (40 $cmH_2O$) and the input pressure was adjusted to obtain a cardiac output of approximately 110 ml $min^{-1}$ $kg^{-1}$ wet body mass. These values were within the physiological range (Shelton and Jones, 1965). Cardiac output, heart rate and aortic pressure were simultaneously measured during the experiments. Hearts that did not stabilize within 10 min from the onset of perfusion were discarded. Ten hearts were discarded (8.8 %). The parameters of cardiac performance under basal conditions were measured after 20 min of perfusion; in the treated hearts, the 20-min control period was followed by a further 20 min period during which hearts were perfused with drug-enriched saline containing a given concentration of $N^G$-nitro-L-arginine methyl ester (L-NAME), Methylene Blue (MB), 8-bromo-cGMP, sodium nitroprusside (SNP) or 3-morpholinosydnonimine (SIN-1) (SNP and SIN-1 were used in a darkened perfusion apparatus to prevent degradation). SNP was added cumulatively from $10^{-7}$ to $10^{-4}$ mol $l^{-1}$ and SIN-1 from $5\times10^{-8}$ to $10^{-5}$ mol $l^{-1}$.

#### *Impairment of the endocardial endothelium by detergent treatment*

When the heart was stabilized in the basal condition after 10–15 min of perfusion, 0.1 ml of Triton X-100 (0.05 % in saline) was introduced through the aortic trunk, to avoid damage to the atrium, using the following procedure: the inflow was closed, the afterload was increased to approximately 7 kPa, and Triton X-100 was injected through a needle inserted into the output cannula. After 3–4 isovolumetric systoles, the inflow was reopened and the outflow was adjusted to the control value, the perfusion being continued with saline. This procedure induced filling of the ventricle as a result of temporary incompetence of the valve. Preliminary experiments with Evans Blue dye showed that, using this procedure, there was no backflow into the atrium. Parameters of cardiac performance were measured after 20 min of perfusion with saline following a stabilization period of 30–35 min from the onset of perfusion. Control experiments with afterload increased to 7 kPa and injection of 0.1 ml of saline instead of Triton X-100 (0.05 %) did not alter heart rate (58±3 beats $min^{-1}$, mean ± S.E.M., $N$=5), cardiac output (112±18 ml $min^{-1}$ $kg^{-1}$) and stroke volume (2.0±0.1 ml $kg^{-1}$) (data not shown), indicating that Triton X-100 *per se* and not the perfusion manipulation affected cardiac pump performance.

In the group of detergent-pretreated hearts tested for drug effects, the 20 min period of perfusion with saline was followed by a further period of perfusion with the drug-enriched saline, after which the performance parameters were measured. In this group, the total duration of perfusion was between 55 and 60 min.

### *Statistics*

The results are expressed as mean values ± one standard error of the mean (S.E.M.). Each heart received only one concentration of the drug being tested, under control conditions, after Triton X-100 exposure or in the presence of L-NAME. Since each heart thus represented its own control, the statistical significance of differences was assessed on actual parameter changes using the paired Student's $t$-test. Comparisons for the cumulative response to SNP and SIN-1 were made using Bonferroni's correction. Percentage changes were calculated as the mean ± S.E.M. of percentage changes obtained from individual experiments.

### *Morphological evaluation*

#### *Characterization of EE*

Isolated working hearts were perfusion-fixed for 10–20 min at room temperature with 4 % paraformaldehyde in a Hepes-buffered solution containing (in mmol $l^{-1}$): $CaCl_2{\cdot}2H_2O$, 1.2; $MgCl_2{\cdot}6H_2O$, 0.5; KCl, 2.7; $KH_2PO_4$, 1.5; NaCl, 136.9; $NaH_2PO_4{\cdot}H_2O$, 8.1; Hepes, 25.0; D-glucose, 5.0; pH 7.2. Tissue samples were rinsed in buffer and then dissected from the ventricular and atrial walls. Tissue samples were stained *en block* for *en face* confocal scanning laser microscopy as previously described (Andries and Brutsaert, 1993). Filamentous actin was stained by Bodipy-phallacidin (Molecular Probes; *N*=4 hearts). The von Willebrand factor (vWF; *N*=2) and constitutive nitric oxide synthase (cNOS; *N*=2) in endothelial cells were labelled using commercial antibodies (polyclonal antibody against human vWF and secondary antibodies coupled to FITC, Dakopatts; polyclonal antibody against a synthetic peptide of a sequence derived from bovine cNOS, amino acids 599–613, Affinity Bioreagents). Stained tissue blocks were mounted in a small chamber on a slide filled with Slowfade (Molecular Probes) and observed with a Biorad MRC-600 confocal scanning laser microscope equipped with an Argon ion laser and using the BHS single-channel filter block.

#### *Viability of the EE after Triton X-100 treatment*

To detect damage to endothelial cells and myocytes in control frog hearts (*N*=2) and after experimental protocols with Triton X-100 (*N*=2), hearts were perfused for 10 min with a saline solution containing $8\times10^{-6}$ mol $l^{-1}$ ethidium homodimer-1 (Molecular Probes). This viability tracer enters only dead cells and binds to DNA and remaining RNA. Unbound tracer was washed away by continuous perfusion with saline. Hearts were perfusion-fixed and processed for *en face* confocal microscopy as described above. Dissected tissue samples were stained for F-actin or with TOPRO, a nuclear stain that allows visualization of nuclei from all cells in cardiac tissue. Double-labelled images were obtained using the dual-channel filter blocks (A1 and A2) of the Biorad MRC-600.

## Results

### *Morphology of the EE in frog heart*

Ventricular and atrial trabeculae were both covered with endothelial cells that were positively labelled for vWF (Fig. 1A–C). Sections through trabeculae revealed that no cells were stained for vWF within the trabeculae (Fig. 1D). *En face* optical sections of the EE showed extensive vWF staining adjacent to labelled nuclei. The shape of the stained structures ranged from small spherical particles to small tubule-like particles and included larger, more amorphous, mainly juxtanuclear structures (Fig. 1B,C). In many sections, broad regions corresponding to the peripheral parts of EE cells were almost completely devoid of staining.

F-actin labelling by Bodipy-phallacidin intensively stained myocytes in the ventricular and atrial trabeculae. Since myocytes and EE cells are very closely apposed, very thin optical sections had to be used to observe the actin filaments in EE cells. In a limited number of EE cells, it was possible to see that the actin filaments formed a thin peripheral band (Fig. 1E) outlining a hexagonal cell shape or a less-regular and more elongated cell shape. Some short, thin actin filaments were present in the endothelial cytoplasm. Nuclei of EE cells were frequently visible as dark circular or oval areas framed by the actin staining in myocytes.

Staining for cNOS was restricted to endothelial cells enveloping the trabeculae in ventricular and atrial tissue. Sections through the trabeculae demonstrated specific staining only in EE cells. *En face* optical sections of EE showed cytoplasmic labelling outlining the circular or oval-shaped nuclei (Fig. 1F). There was usually a densely stained area near the nucleus. Controls in which the primary antibody was omitted or in which polyclonal antibodies were used that did not react with frog tissue showed a low level of background staining throughout the EE and myocardium and a few granule-like structures.

### *Functional impairment of the EE in frog heart*

To assess the viability of cardiac tissue in control hearts and after Triton X-100 treatment, working hearts were, prior to fixation, treated with ethidium homodimer-1, which passes through damaged cell membranes and reacts with DNA and the remaining RNA. Superficial *en face* sections of ventricular trabeculae from control hearts, stained with TOPRO after fixation, showed a regular pattern of circular or oval-shaped nuclei in the green channel (Fig. 2A); no staining was observed in the red channel of the confocal microscope. These nuclei represent viable EE cells. Similarly, sections deeper into trabeculae demonstrated only green highly elongated nuclei of viable cardiac myocytes (Fig. 2B). After actin labelling, myocytes had a normal striation pattern (Fig. 2E). In atria, a few EE cells were occasionally damaged, as shown by the presence of yellow endothelial nuclei in merged dual-channel images (Fig. 2C).

The morphology of frog hearts after Triton X-100 treatment was virtually identical to that of control hearts (Fig. 2D,F). Only very occasionally were damaged EE cells present in ventricular tissue (Fig. 2D). No damaged myocardial cells were observed in ventricular tissue; myocytes had a normal actin pattern (Fig. 2F).

### *Pumping performance: effect of functional impairment of the EE*

Time courses for stroke volume and heart rate are shown in Fig. 3, both under control conditions (*N*=5) and after treatment with Triton X-100 (0.05 %) (*N*=5) in unpaced preparations. In control conditions, the performance of the frog heart was stable for at least 1 h, after which cardiac output decreased linearly (Acierno *et al.* 1994). Within 5 min of treatment with Triton X-100, both $V_S$ and $\dot{Q}$ increased and stabilized at these higher values within 10–15 min. Stroke volume increased by 35±5 ml $kg^{-1}$, $\dot{Q}$ increased by 23±8 % (data not shown) and $f_H$ decreased significantly (by 10±2.7 beats $min^{-1}$) for at least 1 h. In addition, there was a similar decrease of $f_H$ (11±1.6 %) in a series of unpaced experiments with Triton X-100 (*N*=12) in

which the effects of detergent were tested only during the first 20 min of perfusion with saline after Triton X-100 treatment (data not shown).

To avoid changes in performance secondary to changes in heart rate (the 'staircase' effect), the experiments were repeated in paced hearts. Under these conditions, treatment

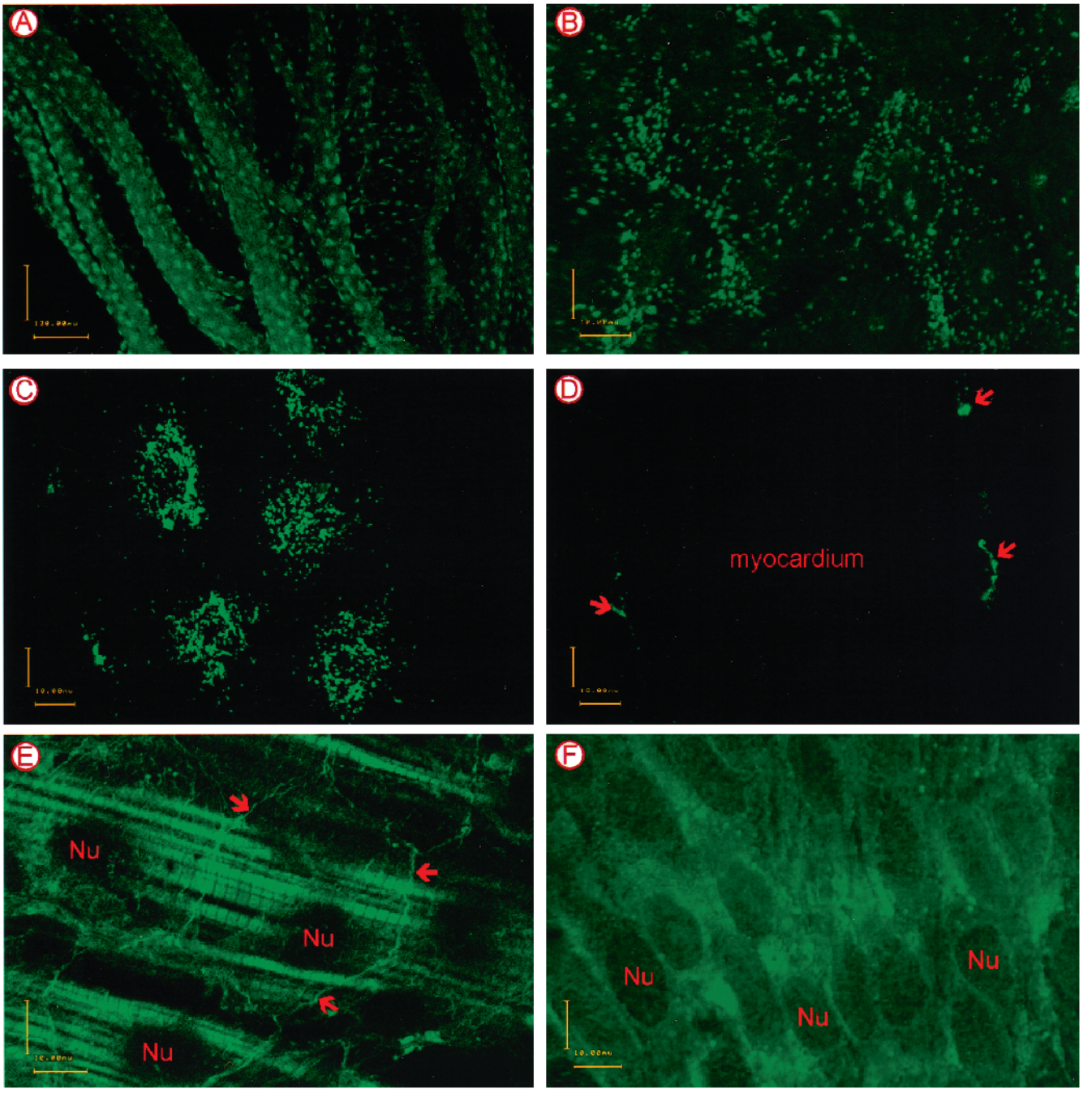


Fig. 1(A–F). Confocal scanning laser micrographs of frog heart after staining of the von Willebrand factor (vWF) (A–D), filamentous actin (E) and constitutive NO synthase (cNOS) (F). Scale bars: A, 130 µm; B–F, 10 µm. (A) Low-power view of atrial trabeculae. Immunostaining of vWF in endocardial epithelium (EE) cells reveals a pattern of regularly distributed labelled spots. The background between the intensively stained spots results from the use of a thick section and increased electronic contrast that augmented the autofluorescence of the tissue. (B) Thin *en face* optical section through the ventricular EE. vWF-stained material is present near the nucleus and has a granular appearance. Long tubular structures were not observed. (C) Detail of atrial EE cells on a thin trabecula. vWF staining is concentrated near the nuclei. Only a few vWF-labelled granules are present in the intracellular regions. (D) Same trabecula as in C, but the focal plane is now 5 µm deeper. Note the vWF staining (arrows) in the EE along the free surface of the trabecula. No staining was observed in the myocardium, the centre of the trabecula. (E) Thin *en face* optical section through the ventricular EE after actin staining. F-actin staining is mainly restricted to the peripheral borders of the EE (arrows), which form a hexagonal pattern. Nuclei (Nu) of EE cells are visible as dark spots against the heavily labelled superficially sectioned myocytes. (F) *En face* optical section through the atrial EE. Cytoplasmic cNOS labelling outlines the EE nuclei. EE cells are elongated.

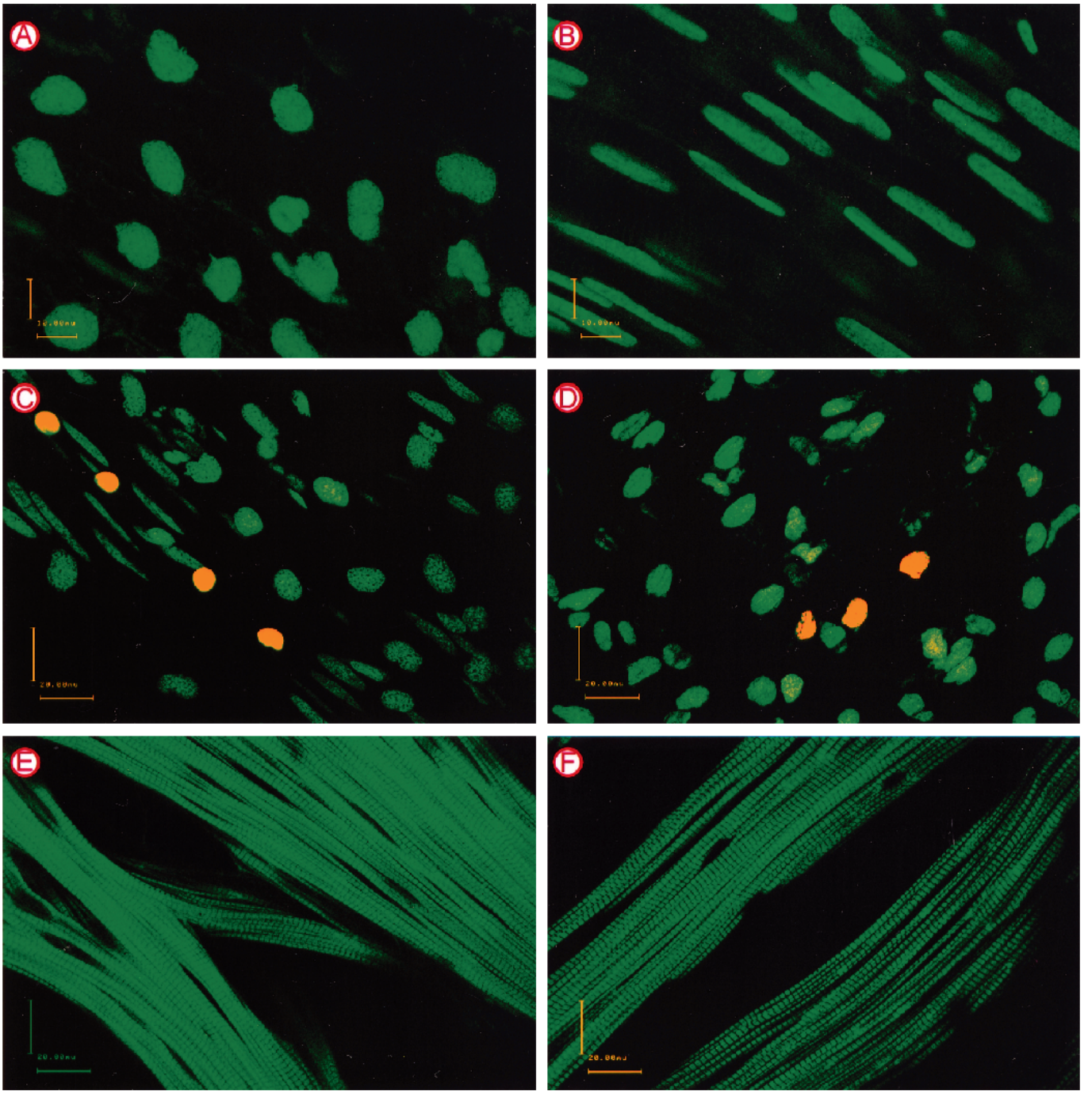


Fig. 2(A–F). Confocal images of control hearts (A–C, E) and of hearts after Triton X-100 treatment (D,F). Prior to fixation, frog hearts were perfused with a solution containing ethidium homodimer-1, a viability tracer that enters dead cells and binds to DNA and remaining RNA. After fixation, tissue strips were stained *en bloc* with TOPRO (A–D), which binds to DNA, or with FITC-phalloidin (E,F), which labels F-actin. All micrographs are dual images obtained by electronically merging images from the 'green' and 'red' channels. Red or yellow nuclei correspond to nuclei from damaged cells. Scale bars: A,B, 10 µm; C,F, 20 µm. (A) Optical section through the ventricular EE showing green nuclei, indicating that the EE cells were viable at the time of fixation. Nuclei from EE cells are circular or oval. (B) Same area as in A, but viewed from a focal plane through the subendocardial myocardium. Nuclei from myocytes are very elongated. The green staining shows that these myocytes were viable. (C) Optical section through control atrial tissue. In most areas, there were only green-stained nuclei, representing viable cells (EE cells have circular nuclei; myocytes have very elongated nuclei). Very occasionally, yellow-stained EE nuclei from dead cells were observed. (D) Optical section through Triton-X-100-treated ventricular tissue. Damaged EE cells were seldom observed; only very occasionally, as in the figure, were a few yellow-stained nuclei from dead EE cells observed. (E,F) Optical sections through the ventricular myocardium from a control heart (E) and from a frog heart after Triton X-100 treatment (F) show an intact actin striation pattern. Ethidium homodimer-1 staining was never observed in cardiomyocytes.

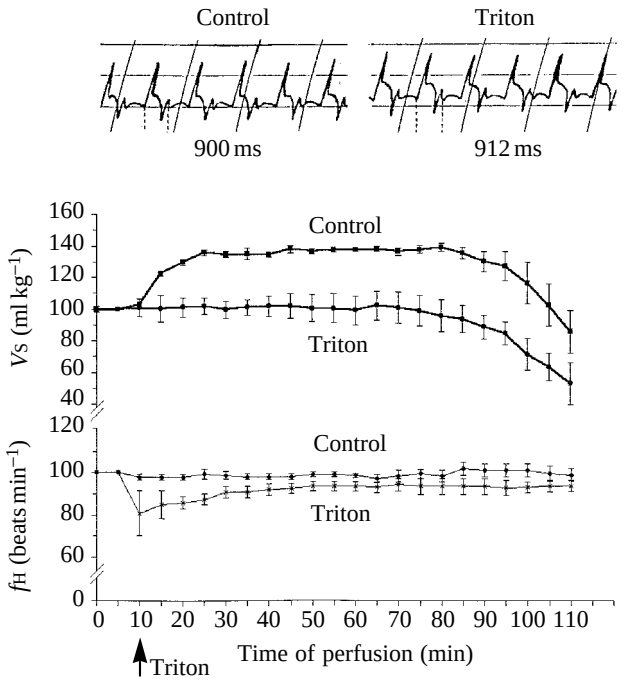


Fig. 3. The upper panels show two typical pressure recording traces under control conditions (left) and after the addition of Triton X-100 (right), with the duration of the systolic phase in milliseconds. The lower panel illustrates the averaged time course of stroke volume ($V_S$) and heart rate ($f_H$) in control ($N$=5) and in Triton-X-100-treated unpaced hearts after approximately 10 min of perfusion ($N$=5); note the stability of the frog heart preparations. Before averaging (mean ± S.E.M.), the data were expressed as a percentage of the value at 5 min of perfusion, i.e. after stabilization. These baseline values were: for the control group, $V_S$=2.3±0.12 ml kg$^{-1}$ and $f_H$=51±2.8 beats min$^{-1}$; for the Triton-X-100-treated group, $V_S$=2.0±0.07 ml kg$^{-1}$ and $f_H$=54±1.4 beats min$^{-1}$.

with Triton X-100 caused a significant increase in cardiac output (from 112 to 121 ml min$^{-1}$ kg$^{-1}$, $P$<0.05); this corresponded to an increase in cardiac output and stroke volume of 14±3.5 %; $W_S$ increased by 12±3.3 % (Fig. 4).

*Exploration of the NO–cGMP pathway in frog heart*

The L-arginine analogue $N^G$-nitro-L-arginine methyl ester (L-NAME) was used to inhibit endogenous NO production in the isolated working frog heart. When L-NAME ($10^{-4}$ mol l$^{-1}$) was administered (Fig. 5A), stroke volume of the paced heart increased by 5.3±2.5 % and stroke work increased by 6±2.6 %. Endogenous NO thus appears to have a mild depressant effect in the frog heart. The stimulatory effect of L-NAME was abolished by prior treatment with Triton X-100 (Fig. 5B).

Since NO activates guanylate cyclase activity, the effect of increased intracellular cGMP levels was mimicked by exogenous administration of 8-bromo-cGMP, a poorly hydrolysable analogue of cyclic GMP (Fig. 6A). Administration of $10^{-6}$ mol l$^{-1}$ 8-bromo-cGMP induced a significant decrease in $V_S$ and $W_S$ (7.9±2.8 % and 9±2.8 %, respectively). Administration of $10^{-6}$ mol l$^{-1}$ Methylene Blue, which at this concentration blocks NO-mediated activation of guanylyl cyclase and therefore decreases endogenous cGMP production, increased stroke volume by 8.5±2.9 % and stroke work by 8.8±3.5 % (Fig. 6B).

SNP, an exogenous NO donor administered in cumulative concentrations (Fig. 7A), significantly depressed the performance of unpaced hearts at $10^{-4}$ mol l$^{-1}$, with a 22±3.6 % decrease in stroke volume, i.e. from 2.0±0.07 to 1.7±0.10 ml kg$^{-1}$, and with a 21±4 % decrease in stroke work, i.e. from 4±0.37 to 3.2±0.35 mJ g$^{-1}$. At this concentration, SNP decreased heart rate by 13±2.8 % ($P$<0.025; $N$=5) (data not shown). In unpaced hearts, the SIN-1 dose–response curve (Fig. 7B) showed that $V_S$ and $W_S$ decreased significantly at all concentrations used without any significant variation in $f_H$ (data not shown). The percentage changes with respect to control values were from 15±1.8 % (at $5\times10^{-8}$ mol l$^{-1}$) to 26±3 % (at $10^{-5}$ mol l$^{-1}$) for $V_S$ and from 16±1.2 % to 30±6 % for $W_S$ at the same concentrations.

In paced preparations, a single administration of $10^{-4}$ mol l$^{-1}$ SNP induced a decrease of stroke volume from 2.0±0.07 to 1.6±0.10 ml kg$^{-1}$ (22±3.2 %) and of stroke work from 4.7±0.27 to 3.6±0.5 mJ g$^{-1}$ (23±4.8 %). The depressant effect of SNP was

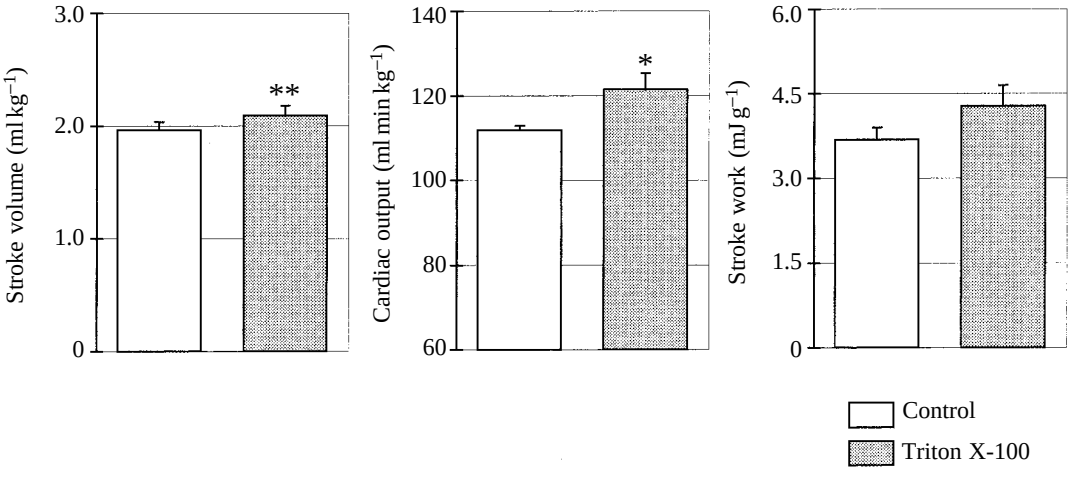


Fig. 4. Effects of Triton X-100 (0.05 %) injections on stroke volume, cardiac output and stroke work in isolated and perfused paced frog hearts. Control values were measured immediately before injection of Triton X-100, and the effect of injection was evaluated 20 min later. Values are means + S.E.M. of 15 experiments. The percentage change from control values was 14.0±3.5 % for stroke volume and 11.8±3.3 % for stroke work. Asterisks mark values that are significantly different from the control value; *$P$<0.05; **$P$<0.01.

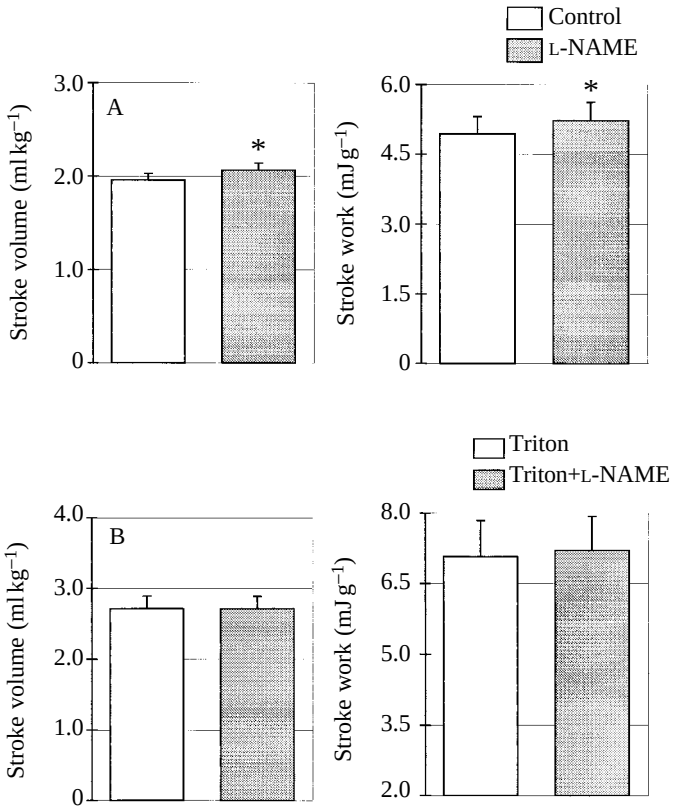


Fig. 5. (A) Effect of $10^{-4}$ mol $l^{-1}$ L-NAME on stroke volume *V*S and stroke work *W*S in isolated and perfused paced frog hearts. Values are means + S.E.M. of 15 experiments. *Significantly different from the control value; $P<0.025$. The percentage changes from control values were 5.3±2.5 % for *V*S and 6±2.6 % for *W*S. (B) Effect of $10^{-4}$ mol $l^{-1}$ L-NAME after treatment with Triton X-100 (0.05 %) on the stroke volume and stroke work in isolated and perfused paced frog hearts. Values are means + S.E.M. of four experiments. There were no significant changes (paired Student's *t*-test: $P=1.0$).

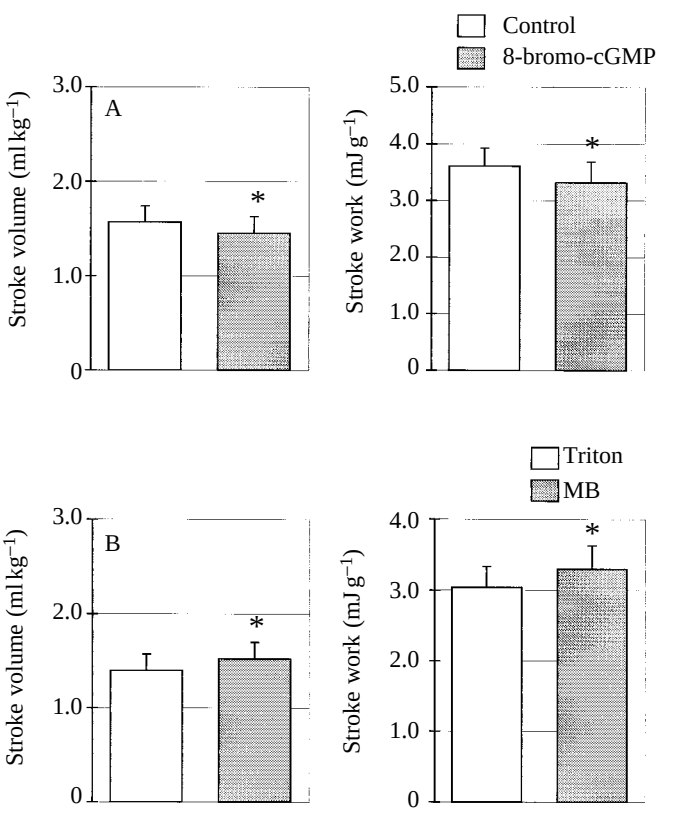


Fig. 6. Effect of $10^{-6}$ mol $l^{-1}$ 8-bromo-cGMP (A) and of $10^{-6}$ mol $l^{-1}$ Methylene Blue (MB) (B) on stroke volume *V*S and stroke work *W*S in isolated and perfused paced frog hearts. Values are means + S.E.M. of five and seven experiments, respectively. *Significantly different from the control value; $P<0.01$. The percentage changes in *V*S from control values were: 8-bromo-cGMP, 7.9±2.8 %; MB, 8.5±2.9 %. The percentage changes in *W*S were: 8-bromo-cGMP, 9±2.8 %; MB, 8.8±3.5 %.

still present, but markedly attenuated, after prior treatment with Triton X-100 or in the presence of $10^{-4}$ mol $l^{-1}$ L-NAME (Fig. 8).

Table 1 illustrates our findings on the duration of the pressure transient or of systole (in ms) measured, as shown in Fig. 3, from the pressure traces. The negative inotropic effects of SIN-1 and 8-bromo-cGMP were accompanied by a reduction in the duration of systole, while L-NAME and MB prolonged systole. Similarly, Triton X-100 also had the effect of prolonging systole.

## Discussion

In the present work, we have carried out a morphological characterization of the avascular heart of the frog, with particular

Table 1. *Duration of the systolic phase*

| Treatment | *N* | Mean duration (ms) | Change in duration (ms) | *P* |
|---|---|---|---|---|
| Control | 50 | 790±19 | – | – |
| Triton X-100 (0.05 %) | 15 | 800 | +10±5 | <0.05 |
| L-NAME (10-4 mol $l^{-1}$) | 15 | 806 | +16±5.8 | <0.01 |
| Methylene Blue ($10^{-6}$ mol $l^{-1}$) | 7 | 820 | +30±12 | <0.025 |
| 8-Bromo-cGMP ($10^{-6}$ mol $l^{-1}$) | 5 | 772 | –18±5 | <0.025 |
| Sodium nitroprusside ($10^{-4}$ mol $l^{-1}$) | 4 | 794 | +4±9.5 | NS |
| SIN-1 ($5\times10^{-8}$ mol $l^{-1}$) | 4 | 756 | –34±9 | <0.01 |

NS, not significant.
L-NAME, $N^G$-nitro-L-arginine methyl ester; SIN-1, 3-morpholinosydnonimine.

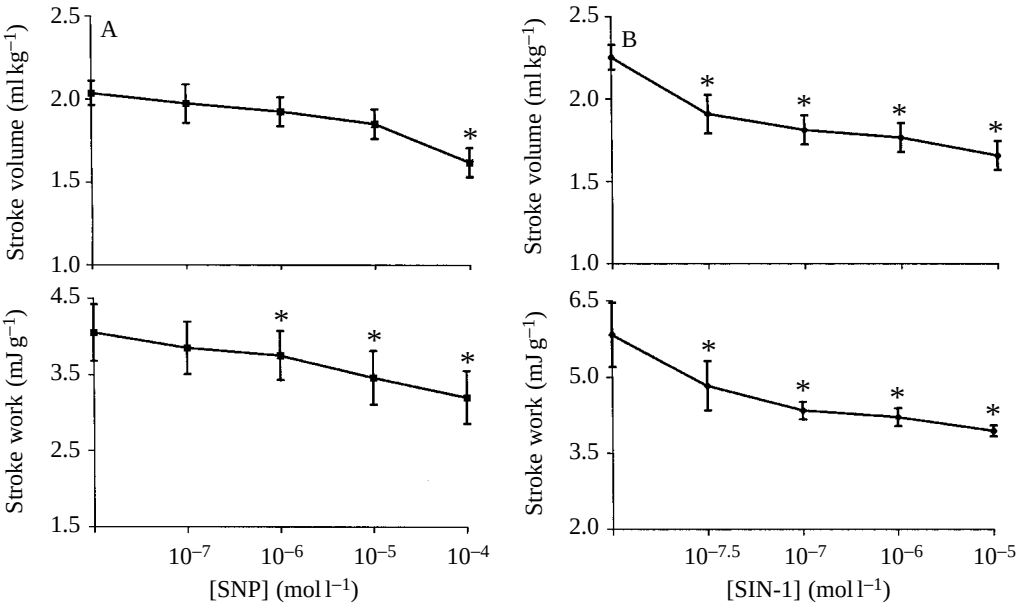


Fig. 7. Dose–response curves for sodium nitroprusside (SNP) (A) and 3-morpholinosydnonimine (SIN-1) (B) on the stroke volume *V*S and stroke work *W*S of isolated and perfused unpaced frog hearts. Values are means ± S.E.M.; *N*=5 for SNP and *N*=4 for SIN-1 experiments. *Significantly different from the control value; *P*<0.025.

reference to cNOS distribution. We have also made a functional evaluation of basal NO production and of its myocardial effects in relation to the specific contribution of the EE. In frog heart, the ventricle covered by the EE is highly trabeculated, resulting in a much higher endothelial surface to myocardial volume ratio than in the compact ventricular wall of higher vertebrates. Moreover, only a thin layer of extracellular material separates the EE cells from the underlying myocytes (Staley and Benson, 1968). As in mammals, the EE cells are characterized by a largely peripheral distribution of F-actin, with vWF localized around the nucleus (Brutsaert and Andries, 1992).

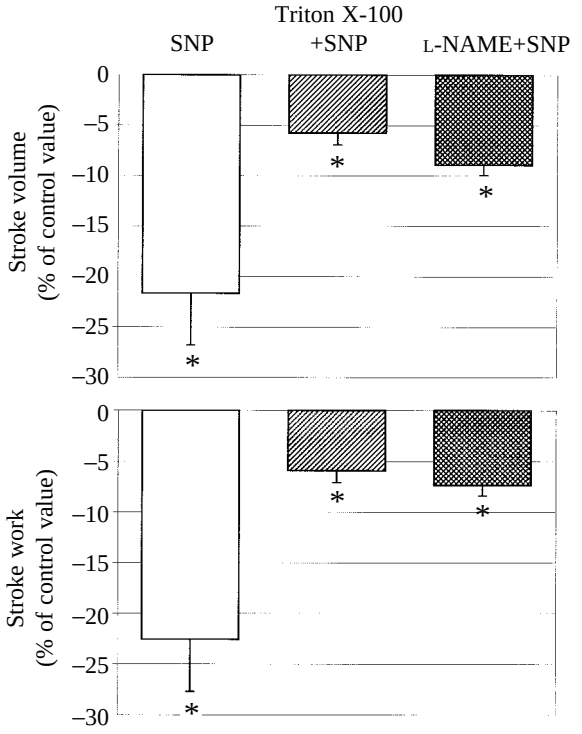


Fig. 8. Effects of sodium nitroprusside (SNP) ($10^{-4}$ mol $l^{-1}$) on stroke volume *V*S and stroke work *W*S in isolated and perfused paced frog hearts, untreated or pretreated with Triton X-100 (0.05 %) or L-NAME ($10^{-4}$ mol $l^{-1}$). Values are means + S.E.M.; *N*=4 for SNP, *N*=3 for Triton X-100+SNP and *N*=3 for L-NAME+SNP. *Significantly different from the control value; *P*<0.025.

Previously, cNOS has been detected in the endocardial and coronary vascular endothelium of rat hearts using the NADPH-diaphorase histochemical technique (Ursell and Mayes, 1993) and by immunohistochemistry (Andries *et al.* 1996). Nitric oxide production by the EE has been demonstrated in cultured EE cells and in isolated cardiac valves of mammalian species (Mohan *et al.* 1996). We believe the current work to be the first demonstration of the presence of cNOS in the EE of the frog heart. Given the very close proximity of the EE and underlying myocytes, cNOS activity in the EE could exert a direct effect on myocardial contractility.

Studies with isolated and perfused mammalian heart preparations have shown that cNOS is associated with the continuous generation of NO at a relatively modest basal level (nanomolar concentrations). Although this basal NO production is considered critical for the preservation of cardiac and vascular homeostasis (Moncada *et al.* 1991), there is no consensus as to the effect of physiological concentrations of NO on heart rate and myocardial contractility in the whole heart. While earlier studies suggested that the inotropic action of NO donors (e.g. SNP) or NOS inhibitors (e.g. L-NMMA) in isolated hearts was secondary to the effects of coronary perfusion (Amrani *et al.* 1992; Fort and Lewis, 1991), the possibility that these contractile effects could in part be due to direct NO diffusion into the myocardium was not excluded. The inotropic action of increased NO levels has been variously reported to be negative (Balligand *et al* .1993; Meulemans *et al.* 1988; Grocott-Mason *et al.* 1994; Paulus *et al.* 1994), positive (Mohan *et al.* 1996; Kojda *et al.* 1996) or absent (Weyrich *et al.* 1994).

These conflicting results may be at least partly explained by

the different levels of performance of mammalian hearts, i.e. isolated unloaded myocyte, papillary muscle or intact heart (*in vitro* or *in vivo*), in association with various levels of sympathetic or parasympathetic tone, myocardial cGMP content (Mohan *et al.* 1996) and interactions between several endothelium-derived mediators such as prostaglandins (Mohan *et al.* 1995).

Here, we demonstrate that the NO donor SNP exerts a negative inotropic effect in a poikilotherm working heart which is paralleled by a positive inotropic effect obtained when NOS activity is inhibited by L-NAME. These inotropic effects are coupled to changes in the duration of the pressure transient, or systolic duration, that correspond to the finding in mammals that cardiac endothelium and the NO–cGMP pathway affect myocardial performance mainly by influencing twitch duration, by shifting the time of onset of relaxation (Brutsaert *et al.* 1988; Smith *et al.* 1991). In frog ventricular myocytes, NO donors, in particular SIN-1, exert a concentration-dependent regulation of cardiac $Ca^{2+}$ current, $I_{Ca}$, controlled by cGMP, and thus linked to the activation of guanylyl cyclase (Mèry *et al.* 1993). The negative inotropic effect of micromolar concentrations of SNP and of the more specific NOS inhibitor SIN-1 may indeed result from inhibition of $I_{Ca}$ by activation of the cGMP-stimulated cyclic AMP phosphodiesterase. Our finding of a negative inotropic effect of the cGMP analogue 8-bromo-cGMP confirms previous data obtained in isolated frog ventricular trabeculae (Singh and Flitney, 1981).

The positive inotropic effect resulting from inhibition of guanylate cyclase by MB may be due to a reduction of cGMP concentration in the preparation. Taken together, these effects demonstrate that, in the isolated frog heart, there is both basal release of NO and basal guanylate cyclase activity. No cNOS staining was observed in the myocardium, but we cannot exclude the presence of cNOS in the epicardium which, however, has a much smaller volume ratio than the EE. Neural NOS, found in nerve cells in the frog heart, occurs mainly in the atria; it is not found in the ventricle (Clark *et al.* 1994). Thus, morphological evidence suggests that the EE cell is the major cNOS-expressing cell type in the frog heart. Consequently, in basal conditions, the EE of the frog heart may produce NO in amounts sufficient to exert a negative inotropic effect on the underlying myocardium.

We used a lower concentration of Triton X-100 than those used in mammalian preparations (Andries *et al.* 1991), because treatment with 0.5 % Triton resulted in ventricular asystole. Treatment with 0.05 % Triton, as in Li *et al.* (1993), affected only the ventricular luminal surface and did not influence the mechanical performance of the atrial myocardium or its endothelial secretory function. However, since substances added to the normal Ringer's solution superfused the entire heart, they might have modulated ventricular performance indirectly through their effect on the mechanical or secretory activity of the atrium or atrial endothelium.

Exposure of the ventricular luminal surface to Triton X-100 did not result in any morphological change in either endothelium or myocardium, but caused a positive inotropic effect and resulted in the loss of response to L-NAME. Thus, exposure to Triton X-100 depressed basal release of NO from the EE. In line with the abolition of vascular endothelium-dependent relaxation induced by Triton X-100 in isolated rat hearts despite the continuing presence of NOS enzyme activity (Panda *et al.* 1996), this depressant effect may be attributable to an interruption of the signal transduction pathway that normally activates cNOS in the EE. The loss of cNOS enzyme activity in the EE after exposure to Triton X-100 could be related to changes in intracellular $[Ca^{2+}]$. An alternative hypothesis is that Triton X-100 could impair the sensing surface of the EE, with a subsequent decrease of stimulation as a consequence of shear strain. Interesting in this context is the report of the selective disappearance of single proteins (e.g. the cholinergic receptors) in isolated preparations and in cell cultures (Marchenko and Saga, 1994). In addition, muscarinic receptors are known to be highly sensitive to their microenvironment, as shown by the loss of antagonist selectivity after detergent solubilization (Hulme *et al.* 1990). Indeed, in the same frog heart preparation, Triton X-100 treatment abolished the inotropic responses to exogenous acetylcholine (Gattuso *et al.* 1995). The frog heart is particularly sensitive to mechanical stresses that induce the release of several factors that have a marked effect on cardiac performance (Singh and Flitney, 1981; Tung and Zou, 1995).

In isolated rat right atria, *N*-nitro-L-arginine ($10^{-4}$ mol $l^{-1}$) and its methyl ester derivative ($10^{-3}$ mol $l^{-1}$) did not exert any chronotropic effect, while the NO donor SIN-1 had a bradycardic effect only at concentrations as high as $10^{-3}$ mol $l^{-1}$ (Kennedy *et al.* 1994). In cultured rat cardiomyocytes, the bradycardic effects of carbachol (Balligand *et al.* 1993) and of interleukin-1 beta (Roberts *et al.* 1992) were inhibited by MB and L-NMMA ($N^G$-monomethyl L-arginine). We show that, while neither MB nor 8-bromo-cGMP significantly influenced isolated frog heart rate, the NO donor SNP, at relatively high concentrations ($10^{-4}$ mol $l^{-1}$), exerted a negative action on cardiac automatism. Intriguingly, Triton X-100 and L-NAME reduced heart rate. A search of the literature failed to provide data that could explain these effects, which appear to contrast with the positive inotropic actions exerted by both the detergent and the NOS inhibitor.

In conclusion, our results suggest that the EE in working frog heart *in vitro* produces NO in amounts sufficient to modulate ventricular performance. Furthermore, the presence of vWF and F-actin in the frog EE suggests that they could also be involved in haemostasis and in transendothelial permeability. The role of the EE as a source of NO and as a cardiac mechanosensor of blood-flow-related forces is still obscure. The different types of ventricular myoarchitecture (compact *versus* trabeculated) and the blood supply (luminal *versus* vascular endothelium) in vertebrates complicates the study of EE control of myocardial performance. The avascular heart of the frog, isolated and working at physiological loads, is a promising tool with which to explore the specific role of the EE, free from the effects of the vascular endothelium.

The authors acknowledge crucial methodological input from the two anonymous reviewers to this paper. This work was supported by a grant from Programma Nazionale Ricerche in Antartide (PNRA) 1993–1995, awarded to B.T.

## References


ACIERNO, R., GATTUSO, A., CERRA, M. C., PELLEGRINO, D., AGNISOLA, C. AND TOTA, B. (1994). The isolated and perfused working heart of the frog, *Rana esculenta*: an improved preparation. *Gen. Pharmac.* **25**, 521–526.

AMRANI, M., O'SHEA, J., ALLEN, N. J., HARDING, S. E., JAYAKUMART, J., PEPPER, J. R., MONCADA, S. AND YACOUB, M. H. (1992). Role of basal release of nitric oxide on coronary flow and mechanical performance of the isolated heart. *J. Physiol., Lond.* **456**, 681–687.

ANDRIES, L. J. AND BRUTSAERT, D. L. (1993). Endocardial endothelium in rat heart: cell shape and organization of the cytoskeleton. *Cell Tissue Res.* **273**, 107–117.

ANDRIES, L. J., KALUZA, G., DE KEULENAER, G. W., MEBAZAA, A., BRUTSAERT, D. L. AND SYS, S. U. (1996). Endocardial endothelium and heart failure. *J. cardiac Failure* **2**, 195–202.

ANDRIES, L. J., MEULEMANS, A. L. AND BRUTSAERT, D. L. (1991). Ultrasound as a novel method for selective damage of endocardial endothelium. *Am. J. Physiol.* **261**, H1636–H1642.

BALLIGAND, J. L., UNGUREANU, D., KELLY, R. A., KOBZIK, L., PIMENTAL, D., MICHEL, T. AND SMITH, T. W. (1993). Abnormal contractile function due to induction of nitric oxide synthesis in rat cardiac myocytes follows exposure to activated macrophage-conditioned medium. *J. clin. Invest.* **91**, 2314–2319.

BRUTSAERT, D. L. AND ANDRIES, L. J. (1992). The endocardial endothelium. *Am. J. Physiol.* **263**, H985–H1002.

BRUTSAERT, D. L., DE KEULENAER, G. W., FRANSEN, P., MOHAN, P., KALUZA, G. L., ANDRIES, L. J., ROULEAU, J. L. AND SYS, S. U. (1996). The cardiac endothelium: functional morphology, development and physiology. *Prog. cardiovasc. Diseases* **39**, 239–262.

BRUTSAERT, D. L., MEULEMANS, A. L., SIPIDO, K. R. AND SYS, S. U. (1988). Effects of damaging the endocardial surface on the mechanical performance of isolated cardiac muscle. *Circulation Res.* **62**, 357–366.

CLARK, R. B., KINSBERG, E. R. AND GILES, W. R. (1994). Histochemical localization of nitric oxide synthase in the bullfrog intracardiac ganglion. *Neurosci. Lett.* **182**, 255–258.

FORT, S. AND LEWIS, M. J. (1991). Regulation of myocardial contractile performance by sodium nitroprusside in the isolated perfused heart of the ferret. *Br. J. Pharmac.* **102**, 351P.

GATTUSO, A., PELLEGRINO, D., MAZZA, R. AND TOTA, B. (1995). Inotropic effects of acetylcholine on frog hearts with intact and damaged endocardial endothelium. *J. Physiol., Lond.* **483**, 185P.

GRANT, R. T. AND REGNIER, M. (1926). The comparative anatomy of the cardiac coronary vessels. *Heart* **13**, 285–317.

GROCOTT-MASON, R., FORT, S., LEWIS, M. J. AND SHAH, A. M. (1994). Myocardial relaxant effect of exogenous nitric oxide in isolated ejecting hearts. *Am. J. Physiol.* **266**, H1699–H1705.

HULME, E. C., BIRDSALL, N. J. AND BUCKLEY, N. J. (1990). Muscarinic receptor subtypes. *A. Rev. Pharmac. Toxicol.* **30**, 633–673.

KENNEDY, R. H., HICKS, K. K., BRAIN, J. E. AND SEIFEN, E. (1994). Nitric oxide has no chronotropic effect in right atria isolated from rat heart. *Eur. J. Pharmac.* **255**, 149–156.

KOJDA, G., KOTTENBERG, K., NIX, P., SCHLUTER, K. D., PIPER, H. M. AND NOACK, E. (1996). Low increase in cGMP induced by organic nitrates and nitrovasodilators improves contractile response of rat ventricular myocytes. *Circulation Res.* **78**, 91–101.

LI, K., ROULEAU, J. L., ANDRIES, L. J. AND BRUTSAERT, D. L. (1993). Effect of dysfunctional vascular endothelium on myocardial performance in isolated papillary muscles. *Circulation Res.* **72**, 768–777.

MARCHENKO, S. M. AND SAGA, S. O. (1994). Mechanism of acetylcholine action on membrane potential of endothelium of intact rat aorta. *Am. J. Physiol.* **266**, H2388–H2395.

MEULEMANS, A. L., SIPIDO, K. R., SYS, S. U. AND BRUTSAERT, D. L. (1988). Atriopeptin III induces early relaxation of isolated mammalian papillary muscle. *Circulation Res.* **62**, 1171–1174.

MÈRY, P. F., PAVOINE, C., BELHASSEN, L., PECKER, F. AND FISCHMEISTER, R. (1993). Nitric oxide regulates cardiac $Ca^{2+}$ current. Involvement of cGMP-inhibited and cGMP-stimulated phosphodiesterases through guanylyl cyclase activation. *J. biol. Chem.* **268**, 26286–26295.

MOHAN, P., BRUTSAERT, D. L., PAULUS, W. J. AND SYS, S. U. (1996). Myocardial contractile response to nitric oxide and cGMP. *Circulation* **93**, 1223–1229.

MOHAN, P., BRUTSAERT, D. L. AND SYS, S. U. (1995). Myocardial performance is modulated by interaction of cardiac endothelium derived nitric oxide and prostaglandins. *Cardiovasc. Res.* **29**, 637–640.

MONCADA, S., PALMER, R. M. J. AND HIGGS, E. A. (1991). Nitric oxide: physiology, pathophysiology and pharmacology. *Pharmac. Rev.* **43**, 109–142.

PANDA, A., GIRALDEZ, R. R., XIA, Y. AND ZWEIER, J. L. (1996). Nitric oxide synthase (NOS) activity and abolishment of endothelium-dependent relaxation. *FASEB J.* **10**, 303.

PAULUS, W. J., VANTRIMPONT, P. J. AND SHAH, A. M. (1994). Acute effects of nitric oxide on left ventricular relaxation and diastolic distensibility in humans. Assessment by bicoronary sodium nitroprusside infusion. *Circulation* **89**, 2070–2078.

ROBERTS, A. B., VOVOVOTZ, Y., ROCHE, N. S., SPROFN, N. B. AND NATHAN, C. F. (1992). Role of nitric in antagonistic effects of transforming growth factor-beta and interleukin-1-beta on the beating rate of cultured cardiac myocytes. *Molec. Endocr.* **6**, 1921–1929.

SHELTON, G. AND JONES, D. R. (1965). Central blood pressure and heart output in surfaced and submerged frogs. *J. exp. Biol.* **42**, 339–357.

SINGH, J. AND FLITNEY, F. W. (1981). Inotropic responses of the frog ventricle to dibutyryl AMP 8-bromo-cyclic GMP and related changes in endogenous cyclic nucleotide levels. *Biochem. Pharmac.* **30**, 1475–1481.

SMITH, J. A., SHAH, A. M. AND LEWIS, M. J. (1991). Factors released from endocardium of the ferret and pig modulate myocardial contraction. *J. Physiol., Lond.* **439**, 1–14.

STALEY, N. A. AND BENSON, E. S. (1968). The ultrastructure of frog ventricular cardiac muscle and its relationship to mechanisms of excitation–contraction coupling. *J. Cell Biol.* **38**, 99–114.

TUNG, L. AND ZOU, S. (1995). Influence of stretch on excitation threshold of single frog ventricular cells. *Exp. Physiol.* **80**, 221–235.

URSELL, P. C. AND MAYES, M. (1993). The majority of nitric oxide synthase in pig heart is vascular and not neural. *Cardiovasc. Res.* **27**, 1920–1924.

WEYRICH, A. S., MA, X., BUERKE, M., MUROHARA, T., ARMSTEAD, V. E., LEFER, A. M., NICOLAS, J. M., THOMAS, A. P., LEFER, D. J. AND VINTEN-JOHANSEN, J. (1994). Physiological concentrations of nitric oxide do not elicit an acute negative inotropic effect in unstimulated cardiac muscle. *Circulation Res.* **75**, 692–700.